Ovine oocytes display a similar germinal vesicle configuration and global DNA methylation at prepubertal and adult ages

Article *in* Theriogenology · July 2019

DOI: 10.1016/j.theriogenology.2019.07.011

CITATIONS
8

READS
25

7 authors, including:

José Luis Alabart
Agrifood Research and Technology Centre of Aragon
125 PUBLICATIONS **2,208** CITATIONS
SEE PROFILE

Belén Lahoz
Agrifood Research and Technology Centre of Aragon
59 PUBLICATIONS **459** CITATIONS
SEE PROFILE

Contents lists available at ScienceDirect

Theriogenology

journal homepage: www.elsevier.com

Ovine oocytes display a similar germinal vesicle configuration and global DNA methylation at prepubertal and adult ages

María J. Cocero [a, *], Pilar Marigorta [a], Fernando Novillo [a], José Folch [b, c], Pilar Sánchez [b, c], José L. Alabart [b, c], Belén Lahoz [b, c]

[a] *Departamento de Reproducción Animal, Instituto Nacional de Investigación y Tecnología Agraria y Alimentaria, Avenida Puerta de Hierro 12 local 10, 28040, Madrid, Spain*
[b] *Unidad de Producción y Sanidad Animal, Centro de Investigación y Tecnología Agroalimentaria de Aragón (CITA), Gobierno de Aragón, Av. Montañana 930, 50059, Zaragoza, Spain*
[c] *Instituto Agroalimentario de Aragón – IA2 (CITA-Universidad de Zaragoza), Spain*

ARTICLE INFO

Article history:
Received 12 February 2019
Received in revised form 20 June 2019
Accepted 16 July 2019
Available online xxx

Keywords:
Antral follicle
Sheep
Chromatin
Epigenetic
Embryo
Blastocyst

ABSTRACT

Epigenetic mechanisms are thought to be involved in the reduced developmental capacity of early prepubertal ewe oocytes compared to their adult counterparts. In this study, we have analyzed the global DNA methylation pattern and *in vitro* meiotic and developmental competence of oocytes at the germinal vesicle (GV) stage obtained from adult and 3-month-old donors. All oocytes were aspirated from antral follicles with a diameter ≥3 mm, and DNA methylation on 5-methylcytosine was detected by immunofluorescence using an anti-methyl cytosine antibody. The main global chromatin configuration pattern shown by both prepubertal and adult ovine oocytes corresponded to condensed chromatin localized close to the nuclear envelope (the SNE pattern). Immunofluorescence showed that a global bright nuclear staining of 5-methylcytosine (5-mC) occurred in all germinal vesicle stage oocytes and matched the propidium iodide staining pattern. The total fluorescence intensity values of lamb GVs were not lower than those observed in adult GVs. The meiotic competence and cleavage rates were similar in adult and prepubertal oocytes, however, the developmental competence of embryos to reach blastocysts was higher for adult oocytes than lamb oocytes ($p<0.0001$). In conclusion, our results indicate that adult-size oocytes derived from 3 to 4 month old prepubertal ewes show similar GV morphology and DNA methylation staining patterns to those obtained from adult animals, despite exhibiting a lower developmental competence.

1. Introduction

Juvenile *in vitro* embryo transfer constitutes a cost-effective method for multiplying desirable sheep genotypes in breeding programs [1–3]. Oocytes from prepubertal and adult sheep differ in their capacity for *in vitro* embryo development [4,5], however, it has been assessed that the pregnancy rates for recipient ewes were similar for both juvenile (57%) and adult (61%) oocytes [6]. Most of the studies undertaken with oocytes derived from prepubertal sheep as a model for oocytes with low developmental competence have used 30–40-day-old lambs as donors, although oocyte competence, measured in terms of developmental ability to reach the blastocyst stage, increases with donor age in lambs and is higher at 6–7 weeks of age than at 3–4 weeks of age [7]. Diverse studies reporting lower developmental rates in ovine *in vitro* production (IVP) using prepubertal oocytes have pointed out perturbed cytoplasmic maturation [4,5,7–9] and altered DNA methylation patterns [10,11] as possible causes for the reduced oocyte competence, however, the involvement of DNA methylation is still debated [12]. The crucial effect of oocyte quality on developmental outcomes might be mediated by maternal factors stored in the oocyte, including subcellular macromolecules and organelles; lower developmental competence is associated with deficiencies in the mRNAs stored during oocyte growth [8] and also with mitochondrial distribution and functionality [9]. These factors are essential for embryo development, especially before the maternal-to-embryonic transition, and accumulate in oocytes during the course of folliculogenesis and oogenesis [13] while the chromatin in the oocyte nucleus (germinal vesicle: GV) is decondensed. Meiotic competence is acquired during the later stages of folliculogenesis and is accompanied by a progressive silencing of transcription and profound structural changes in the chromatin within the oocyte nucleus [14,15].

Oocyte meiosis is characterized by a prolonged pause at the diplotene stage called dictyate. Oocytes remain at the dictyate stage until LH induces final oocyte maturation [16]. Primordial follicles become activated and are continuously recruited in cohorts to initiate folliculogenesis [17]. Meiotic competence is acquired during folliculogenesis, accompanied by a progressive silencing of transcription and profound structural changes in chromatin for the control of gene expression within the oocyte nucleus [14,15]. These changes include not only local chromatin modifications at specific promoter regions

* Corresponding author.
Email address: cocero@inia.es (M.J. Cocero)

https://doi.org/10.1016/j.theriogenology.2019.07.011
0093-691/

and cis-acting regulatory elements of single copy genes, but also large-scale chromatin remodeling throughout large sections of the genome. Failure to establish correct germline-specific DNA methylation patterns has serious consequences for post-fertilization development [18]. DNA methylation is required for successful chromosome synapsis in oocyte prophase, and reduced DNA methylation levels are associated with defects in chromosome synapsis during meiosis in both male and female germ cells [19]. Studies have suggested that methylation imprinting is acquired after birth during the growth phase of diplotene-arrested oocytes [20]. In parallel with DNA methylation changes, the functional differentiation of chromatin structure during post-natal oocyte growth is essential for the control of transcription, nuclear architecture, the establishment of gamete-specific DNA methylation patterns, and the maintenance of chromosome stability during meiosis [21]. This process of epigenetic maturation is strictly required for the acquisition of both meiotic and developmental potential [22], and chromatin configuration represents a morphological marker of oocyte differentiation and competence [reviewed in [23]].

The modifications in large-scale chromatin configuration during oocyte growth in adult sheep have been well documented [24]. In detail, all oocytes isolated from preantral follicles display highly dispersed chromatin in the nucleoplasm, with a typical non-surrounded nucleolus (NSN) configuration. Later, during the growing phase, a condensed chromatin surrounding the nucleolus (surrounded nucleolus –SN- pattern) starts to appear and characterizes sheep oocytes of 110 ± 10 μm isolated from early antral stage follicles. Medium and pre-ovulatory antral follicles develop a new pattern of GV organization where the condensed chromatin is localized around the nucleolus and close to the nuclear envelope (SNE pattern) [24].

In contrast to adult oogenesis, prepubertal oogenesis remains poorly characterized in sheep. Pioneering experimental results [10] showed that the genome-wide methylation status, expressed as the percentage of methylated *vs*. total DNA, was significantly lower in adult-size lamb oocytes than in those from adult sheep. The study also showed that oocytes from 4-week-old lambs with a similar diameter to that of adult oocytes still displayed transcriptional activity and lacked nuclear competence. Along a similar line, Fang et al. [11] recently reported no signal for 5-mC fluorescence in lamb GVs using hormonally treated early prepubertal donors. In striking contrast, Masala et al. [11] reported no differences in global DNA methylation between adult and 4-week-old prepubertal donors. To the best of our knowledge, no studies on more advanced prepubertal ages have been published for ovine species, even though it has been shown that in mice, the proportion of SN and NSN antral oocytes changes dramatically with female aging [25], and despite the high availability of slaughterhouse ovaries in countries that consume prepubertal ewe lambs.

Considering the important genetic and economic advantages of using juvenile domestic animals, and that fully-grown GV oocytes must change from a NSN configuration before gaining full meiotic competence and halt gene transcription before having the capacity to sustain blastocyst formation [26], the aim of the present study was to address the following issues: (a) to identify nuclear features and the functionality of prepubertal oocytes obtained from 3–4-month-old ewe lambs and quantify their relative intensity of global DNA methylation by immunostaining with a 5-mC antibody; (b) to compare GV architecture and DNA methylation of ovine oocytes from follicles ≥ 3 mm in diameter in adult and lamb ewes; and (c) to assess *in vitro* embryo production with prepubertal- and adult-derived oocytes, at the same time and under the same experimental conditions.

2. Material and methods

Unless otherwise stated, all chemicals were purchased from Sigma Aldrich Quimica S.A (Madrid, Spain).

2.1. Experimental design

The aims of this study were addressed in two different experiments conducted in two successive years.

Experiment 1 was carried out to characterize the morphological traits and DNA methylation (5′CpG) fluorescence patterns at the GV stage of prepubertal (3–4 months old) oocytes from follicles ≥ 3 mm in diameter in a large and heterogeneous sample of sheep. This experiment involved 12 replications during 1 year. A total of 440 selected prepubertal cumulus-oocyte complexes (COCs) were distributed as follows: 130 to measure oocyte size, 106 for GV configuration and DNA methylation studies, and 204 for the assessment of meiotic competence.

Once the DNA methylation patterns had been characterized in prepubertal GVs, experiment 2 was performed to test whether the developmental differences after *in vitro* production (IVP) between ewe lambs and adult ewes were congruent with nuclear architecture. For this purpose, ovaries of adult and prepubertal sheep where collected on the same day; IVP and nuclear architecture observations were performed at the same time and under the same experimental conditions using 160 adult and 199 prepubertal grade 1 COCs. Random samples of oocytes from adult (24) and lamb (28) ewes were collected for GV measurements, and the rest were used to verify meiotic competence and development to the blastocyst stage after *in vitro* fertilization (IVF).

In these two different experiments, the same methodologies were used as described below.

2.2. Oocyte collection

Ovaries were obtained from a local abattoir from adult and prepubertal (3–4 months old) ewes. The ovaries were washed and transported to the laboratory at 33 °C in saline solution (9 g/L NaCl) supplemented with 306 mg/L penicillin G (P3032) and 680 mg/L streptomycin (S1277). Follicle aspiration was performed 2–4 h after slaughter.

The oocytes were obtained following a previously described method [27]. COCs were aspirated from follicles ≥3 mm in diameter using a 21 G (gauge) needle mounted on an COOK IVF aspiration pump (Brisbane, QLD, Australia) using a vacuum pressure (−25 mmHg) and collected in a 15 mL Falcon tube (Becton Dickinson, Madrid, Spain) with 1 mL of TCM199 supplemented with 40 μg/mL gentamicin sulfate, 10 mM 4-(2-hydroxyethyl)-1-piperazineethanesulfonic acid (HEPES), and 10 UI/mL heparin. During aspiration, the collecting tube was maintained at 34 °C. Only COCs with oocytes larger than 120 μm in diameter and showing a homogenous cytoplasm were selected for the experiments.

2.3. Oocyte size measurement

The mean oocyte diameter (*zona pellucida* excluded) was calculated from equatorial sections using a computerized image analysis system (NIS elements-D software, Nikon, Tokyo, Japan) connected to a Nikon Eclipse TE 300 inverted microscope and a TV monitor, at 40× magnification.

In experiment 1, the diameter of the oocytes was measured in a sample of 130 COCs from the total selected for *in vitro* maturation (IVM) immediately after recovery, using oocytes with high definition in the digitalized images.

In experiment 2, cytoplasmic diameters were manually measured from the digitalized images of the 24 adult and 28 prepubertal oocytes used for immunofluorescent measures.

2.4. Immunocytochemical staining of oocytes

Immunostaining of DNA methylation was performed following the procedures of Santos & Dean [28] with minor modifications. Cumulus-free oocytes were washed in Dulbecco's phosphate-buffered saline (D-PBS) without Ca and Mg but supplemented with 0.4% bovine serum albumin (BSA) and fixed for 1 h with 2.5% paraformaldehyde before permeabilization with 0.1% Triton X-100 for 30 min. The oocytes were exposed to 4 N HCl for 10 min at room temperature (~25 °C) for depurination, which was blocked by incubation in PBS containing 2% BSA and 0.1% Tween-20 for 30 min. The samples were preserved overnight at 4 °C in 1% BSA and 0.05% Tween-20 in PBS. The oocytes were incubated in a 1:500 dilution of anti-5-mC mouse monoclonal antibody (Calbiochem 162 33 D3, Cat No NA81, San Diego, USA), at 4 °C overnight. The oocytes were washed three times in blocking solution before incubation for 3 h in a 1:500 dilution of the secondary antibody, a donkey anti-mouse IgG (H + L) coupled to Alexa 488 (A-21202, Molecular Probes, Eugene, USA). The DNA was visualized by counterstaining the oocytes with 100 µg/mL propidium iodide (PI) (P-1304, Molecular Probes) for 8 min, followed by ribonuclease A (R4642) treatment (100 µg/ml for 20 min at 27 °C), and the samples were then washed with 0.05% Tween-20. Negative controls were prepared following the same protocol but omitting the primary antibody.

2.5. Digital imaging microscopy

Observations were performed using an inverted epifluorescence microscope (Nikon Eclipse TE 300, Tokyo, Japan) equipped with a CFI Plan Fluor DLL 40× objective, with a numerical aperture (NA) of 0.75 and a working distance (WD) of 0.66 mm; an LED-based Fluorescence Microscope Illuminator pE-100WHT (ESPRIMO 310PE300WDSB-20E20, Tokyo, Japan); a DS-U3 digital camera head (monochrome, 1.50 megapixels, and 4096-level grayscale) and a DS-U3 digital camera control unit (Nikon) interfaced to a computer workstation provided with an interactive and automatic image analyzer (NIS-D Elements software, Nikon). Immunostained oocytes were observed using excitation wavelengths of 490 nm (for Alexa 488) and 535 nm (for PI). For all digital images, the same gain, black level, aperture parameters, time of exposure, and fluorescence parameters were used. A limited number of samples were analyzed using laser confocal microscopy (TCS SP2; Leica Microsystems, Wetzlar, Germany) to compare nuclear architecture detection by inverted microscopy and confocal microscopy. Digital optical sections were obtained at 40× magnification by scanning 1 µm sections of the sample in the z-axis throughout the plane of focus containing the GV equatorial plane (±15 µm). All images were acquired maintaining similar gain and laser parameters.

When mounting oocytes onto slides, attention was paid to ensure that the oocytes on different slides were compressed to the same extent. Therefore, oocytes were mounted in groups of 8–10 in one 15 µL drop of hard mounting medium and covered with a 12 mm diameter coverslip without compression. The coverslip was carefully placed over the drop in such a way that the mounting medium completely reached the edge of the coverslip. Mounting was carried out always by the same person. Under these conditions, the distance between the coverslip and the slide was estimated to be approximately 132.6 µm, which is within the range of diameters of most of the ovine oocytes observed in the present study (103.5–160.1 µm). The estimation of the distance was made by solving for h (the height) in the cylinder volume formula: $V = h \cdot \pi \cdot (D/2)^2$, where D is the diameter of the coverslip (12 mm) and V is the volume of the cylinder (15 mm^3). For each experimental series, all images were acquired with identical settings under fixed thresholds across all slides. For image analysis, the nucleus of each oocyte was selected as the region of interest (ROI) by manually outlining each nucleus. The image analysis software (NIS-Elements) performed two types of measurements: morphometric features (related to dimensions and shape) and fluorescence-related features, as per NIS-Elements manual instructions [29] (Laboratory Imaging s.r.o., Za Drahou 171/17, Cz-102 00 Praha 10). The morphometric features selected to define the GV architecture were: area, diameter, and shape factor. The area was expressed in μm^2 and was calculated from the number of pixels within the ROI. The perimeter (Per) was expressed in µm and represented the total boundary measure Equivalent diameter (EqD) was expressed in µm, and it was defined as the diameter of a circle with the same area as the measured object, applying the formula: $EqD = (4*Area/\pi)^{1/2}$. The shape factor (SF) was a non-dimensional feature and defined whether the object was rough or not. The maximum value of SF was 1, corresponding to a perfect circle. The fluorescence-related features for describing DNA global methylation were total fluorescence relative intensity (TFI) and the mean, maximum, and minimum intensity of fluorescence (MeanI, MaxI, and MinI, respectively), which were expressed as arbitrary fluorescence units (AFUs). We must stress that these immunolocalization analyses, similar to those reported in previous articles on ovine GVs (10, 12), provide an indirect measurement of global DNA methylation (global methylation patterns) and are not meant to precisely quantify the amount of 5-mC in the whole genome or at specific sequences. Several pieces of evidence have demonstrated that chromatin organization [20–22] and global DNA methylation [18,19] are crucial to define oocyte developmental competence, even though information on the exact timing of these process during oogenesis remains unknown in ovine species.

2.6. In vitro maturation (IVM)

COCs with a compact cumulus and homogeneous cytoplasm were placed into maturation medium (30–40 COCs/500 µL) in four-well plates (Nunclon® Fisher Bioblock, Madrid, Spain). The IVM medium consisted of TCM199 + 16 mIU/mL ovine follicle-stimulating hormone (FSH) (F8174) + 7.8 mIU/mL ovine luteinizing hormone (LH) (L5269) + 10 ng/mL EGF + 100 µM cysteamine + 10% (v/v) inactivated fetal calf serum (FCS) (F4135) + 40 µg/mL gentamicin sulfate. The plates were incubated at 38.5 °C in 5% CO_2 in humidified air for 24 h.

2.7. Assessment of oocyte meiotic maturation

After 24 h of culture, the oocytes were mechanically denuded of surrounding cumulus cells by gentle pipetting with a small-bore pipette and washed three times in D-PBS. After IVM, random samples of adult and prepubertal COCs were fixed for 30 min in 2.5% paraformaldehyde and used for the determination of nuclear stage by staining with Hoechst 33342 (20 µM in D-PBS for 20 min). The oocytes were mounted in groups of 8–10 (as detailed in 2.4 section)

and covered with a 12 mm diameter coverslip for epifluorescence microscopic evaluation at 200 to 400× magnification.

2.8. In vitro fertilization (IVF)

After IVM, the oocytes were further morphologically evaluated under transmitted light. Only oocytes with a slightly granulated or homogeneous cytoplasm were selected for IVF. These oocytes were placed into equilibrated fertilization medium composed of synthetic oviductal fluid (SOF) + 20% (v/v) heat-inactivated estrous sheep serum. Fresh semen from one Manchega breed tested ram was used in all the experiments. Capacitation was carried out by a slight modification of the method described previously [5]. Semen was diluted 1:10 (v/v) in SOF + 0.3% BSA + 40 µg/mL gentamicin sulfate and centrifuged at 200 × *g* for 5 min. Two aliquots were collected for counting and the subjective evaluation of progressive individual motility. Since the semen was of high quality, it was not processed further. The pellet was diluted with fertilization medium at a final concentration of 1×10^6 total sperm/mL. The oocytes and sperm were subsequently incubated in 50 µL drops containing a maximum of 15 oocytes, under Nidoil oil (Nidacon NO-300, Sweden), in four-well dishes (Nunclon®, Fisher Bioblock) at 38.5 °C in a humidified atmosphere with 5% CO_2 for 24 h.

2.9. In vitro culture (IVC)

Presumptive zygotes were cultured to the blastocyst stage in Petri dishes containing 30 µL droplets of SOF supplemented with essential (B6766) and non-essential (M7145) amino acids, 40 µg/mL gentamicin sulfate, and 0.4% BSA fatty acid-free (A0281) under Nidoil oil in a humidified atmosphere with 5% CO_2, 5% O_2, and 90% N_2. The number of cleaved oocytes was recorded at 48 h after IVF. The embryos were incubated for 8 d at 38.5 °C. At 3 and 5 d after IVF, half of the medium (15 µL) was replaced with 15 µL SOF supplemented with 20% and 10% (v/v) FCS, respectively, in order to obtain, from day 3 onwards, a FCS concentration of 10% (v/v). The blastocyst rates were assessed on days 7 and 8 after IVF.

2.10. Statistical analysis

The percentages of *in vitro* maturation, fertilization and development were compared using an ANOVA for categorical variables using the categorical modeling procedure (PROC CATMOD) of SAS [30]. Due to the expected presence of outliers, the correlations of morphometric and fluorescence variables were assessed using the Spearman rank-order correlation coefficients using PROC CORR of SAS. Regression analyses, analysis of variance (ANOVA), and analysis of covariance (ANCOVA) were performed by means of robust methods using PROC ROBUSTREG of SAS. The main purpose of these methods is to detect outliers and provide resistant (stable) parameter estimates in the presence of outliers by limiting their influence on parameter estimations and statistical significance. The regression line between the total relative fluorescence intensity and the area of GVs from prepubertal immature oocytes was calculated by MM estimation. Outliers and leverage points from the regression line, which were estimated by robust methods, were identified and studied. Comparisons of morphometric and fluorescence features of immature GVs from adult and prepubertal ewes were carried out using a robust ANOVA (M estimation). For the fluorescence features, models including each morphometric feature as a covariate were also considered.

3. Results

3.1. Experiment 1: Nuclear features and meiotic competence of oocytes from 3–4-month-old prepubertal ewes

3.1.1. Oocyte size

The mean diameter and standard deviation (SD) of oocytes in a random sample of 130 COCs from the total COCs selected for IVM after recovery was 124.7 ± 6.5 µm, with a range from 109.9 to 147.1 µm.

3.1.2. GV chromatin configurations and global DNA methylation (5-mC) of prepubertal oocytes

The immunofluorescence analysis showed that a global bright nuclear staining of 5-mC (green fluorescent signal) was present in all prepubertal oocytes evaluated in Experiment 1 (n = 106), confirming an established genome-wide methylation in oocytes from follicles ≥ 3 mm in diameter. The methylation (5-mC antibody) and DNA (PI) signals were exactly coincident in the GVs (Fig. 1).

Even though immunolabeling revealed global DNA methylation in all oocytes analyzed, noticeable differences were perceived in both the chromatin condensation and DNA methylation between individual oocytes (Table 1). Although the immunofluorescent signal showed high variability between oocytes, the TFI was high enough to detect the global chromatin configuration in all oocytes. The shape of the oocyte nucleus in Fig. 1 was the most frequent (>90%), with a global chromatin structure of condensed DNA localized in close apposition to the nuclear envelope (SNE); this configuration is very similar to that previously described in adult sheep oocytes obtained from antral follicles ≥ 3 mm in diameter [24]. The SN pattern was only detected in 2 out of the 106 oocytes analyzed (Fig. 2 C and 2 D).

The morphological features also showed a significant correlation ($p < 0.01$) with the fluorescence features, except for the SF, which was only significantly correlated with the total fluorescence intensity. In particular, size was positively correlated with the total relative fluorescence intensity, whereas negative correlations were found between size and both the mean and the minimum intensity features

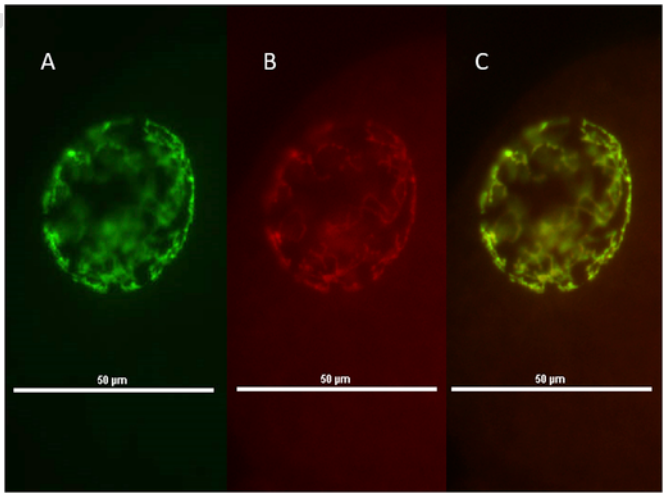

Fig. 1. Methylated prepubertal oocyte nucleus stained with A) anti-5-methylcytosine antibody (green), B) propidium iodide (red), and C) overlay (yellow). Area: 1309.1 μm^2; total fluorescence intensity: 52.9×10^6 AFU. . (For interpretation of the references to colour in this figure legend, the reader is referred to the Web version of this article.)

Table 1
Morphometric and fluorescence intensity measurements in prepubertal ewe oocytes from antral follicles ≥3 mm in diameter (n = 106 oocytes).

Variable	Range	Mean ± SD	Median
Morphometric features			
Area (μm^2)	125.5–3246.3	1306.1 ± 557.7	1280.0
EqD (μm)	12.6–64.3	39.8 ± 9.1	40.4
Per (μm)	42.3–206.0	129.3 ± 28.6	129.8
SF	0.600–0.988	0.956 ± 0.044	0.968
Fluorescence features[a]			
TFI (× 10^6)	6.2–130.1	45.3 ± 20.6	46.5
MinI	158–1024	337.7 ± 143.3	310.5
MeanI	242.9–3278.9	1016 ± 562.1	905.8
MaxI	417–4095	3294.6 ± 1139.0	4095

[a] Expressed in arbitrary fluorescence units (AFU). **EqD**: Equivalent diameter; **Per**: Perimeter; **SF**: Shape factor; **TFI**: total intensity of fluorescence; **MinI**: minimum intensity of fluorescence; **MaxI**: maximum intensity of fluorescence.

(Table 2). In other words, GVs with a bigger size had a higher total relative fluorescence intensity and lower mean and minimum intensity values than those smaller in size. The highest correlations observed between fluorescence and morphometric features were those of TFI with either the area or the equivalent diameter ($\rho = 0.567$; $p<0.01$ for both). The relationship between TFI and GV area is displayed in Fig. 3. Despite the high variation observed in TFI as well as in area, most GVs (100/106) fell near the regression line estimated by robust methods and displayed condensed chromatin close to the SNE; the nucleolus was no longer displayed in this final pattern of the GVs. Three GVs identified as outliers and/or leverage points and represented as dots inside diamonds can be seen in Fig. 2 A, E and F. Fig. 2 A was the smallest one in experiment 1, showing an atypical configuration and was considered as rare. The GV in Fig. 2 B, E and F displayed the typical SNE pattern and showed higher values for area and TFI.

Confocal single z-sections of methyl-CpG staining with Alexa fluorophore (Suppl. Fig. 1) confirmed that the pattern of a ring of compacted chromatin around the nucleolus was not detected in the majority of the full-grown prepubertal ewe oocytes. Instead, a GV organization where the condensed chromatin appeared localized close to the nuclear envelope (i.e., a fluorescent circle leaving a center without fluorescent signal) was the most common pattern (SNE).

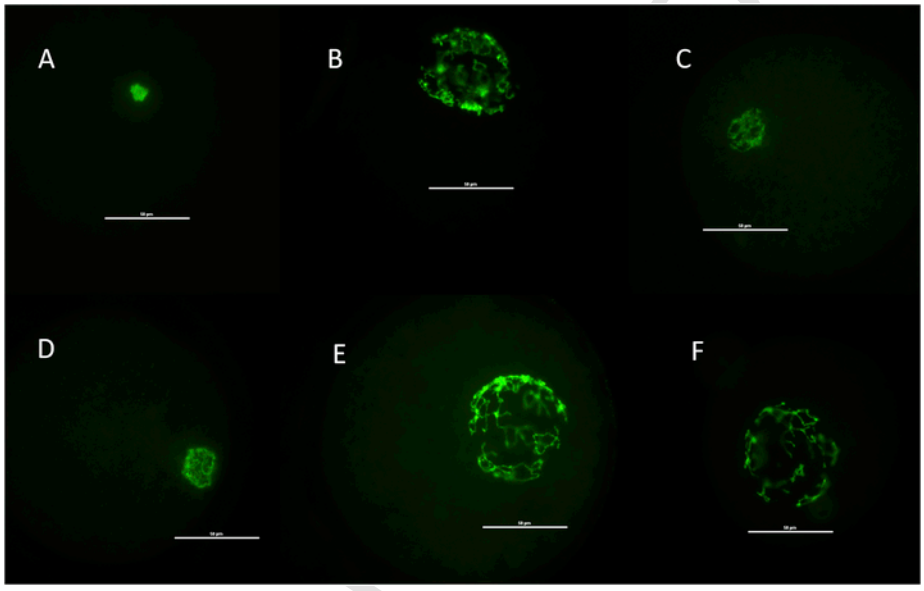

Fig. 2. Configurations of germinal vesicles (GVs) observed after immunolabeling of 5-methylcytosine of prepubertal sheep oocytes. A: GV with the smallest area (125.5 μm^2) and highest mean fluorescence intensity (3278.9 AFU). B: GV with the lowest mean fluorescence intensity (242.9 AFU). C and D: oocytes showing a surrounded nucleus (SN) configuration of the GV, with a very similar small area (441.9 μm^2 and 403.5 μm^2, respectively). E and F: oocytes showing GVs with a similar large size (2938.5 μm^2 and 2657.1 μm^2, respectively) and total fluorescence intensities that differ greatly (130 × 10^6 and 51.9 × 10^6 AFU, respectively).

Table 2
Spearman's correlation coefficients between morphometric and fluorescence intensity in prepubertal ewe oocytes (n = 106).

Morphometric features					Fluorescence features			
	Area	EqD	Per	SF	TFI	MinI	MeanI	MaxI
Area	–	0.999 **	0.991 **	0.330 **	0.567 **	−0.409 **	−0.363 **	0.059
EqD		–	0.991 **	0.330 **	0.567 **	−0.409 **	−0.364 **	0.059
Per			–	0.248 *	0.544 **	−0.439 **	−0.384 **	0.045
SF				–	0.342 **	0.142	−0.005	0.078
TFI					–	0.225 *	0.454 **	0.714 **
MinI						–	0.752 **	0.509 **
MeanI							–	0.777 **
MaxI								–

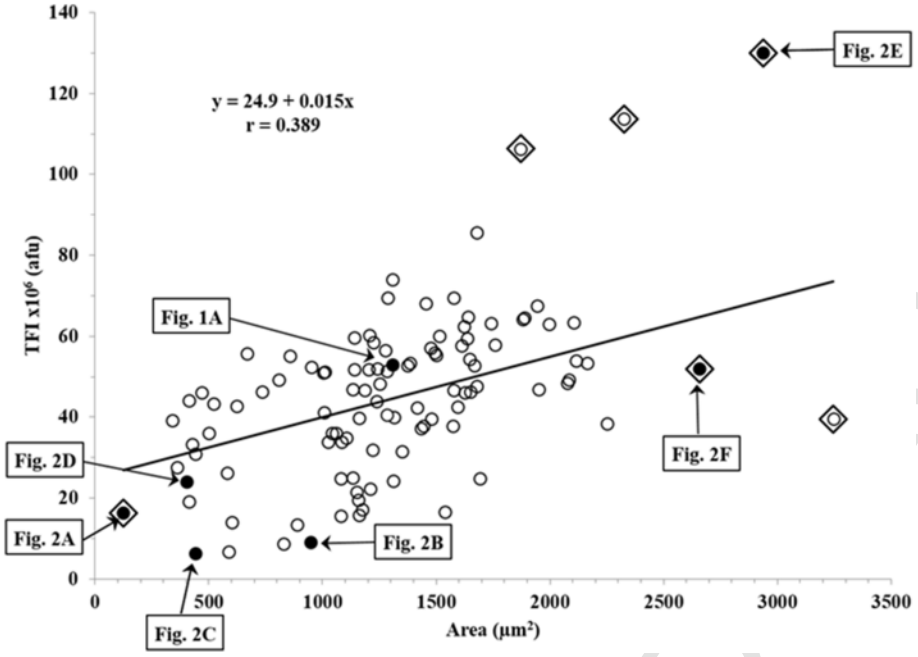

Fig. 3. Relationship between the total fluorescence intensity and the area of the germinal vesicle in prepubertal ewe immature oocytes. Black dots correspond to germinal vesicles that are shown in Figs. 1 and 2, referenced by the corresponding number and capital letter. Dots inside diamonds represent outliers and/or leverage points.

3.1.3. Meiotic competence of oocytes from prepubertal follicles ≥3 mm

Most oocytes aspirated from antral follicles ≥3 mm restarted meiosis (94.1%; Table 3), however, only 74.01% reached the metaphase II (MII) stage at 24 h and 20.1% stopped at the MI stage, which might indicate delayed nuclear maturation kinetics.

3.2. Experiment 2: morphological and functional differences between GVs of adult and prepubertal oocytes

3.2.1. Oocyte size

The mean diameter and standard error of 24 adult and 28 prepubertal oocytes was 123.6±2.2 and 133.8±2.0 µm, respectively, with a range from 103.5 to 136.5 µm in adult and 106.4–160.1 µm in prebubertals. The measures of GV area and diameter were both higher ($p<0.005$) for prepubertal than adult oocytes (Table 4).

3.2.2. Chromatin configurations and global DNA methylation of prepubertal and adult GVs

Immunopositivity for 5-mC was detected in all the 24 adults and 28 lamb ewe GVs that were immunolabeled with the anti-methylcytosine antibody, showing that both prepubertal and adult ewe oocytes from follicles ≥3 mm exhibit a genome-wide methylation pattern.

Table 3
Percentage of ovine prepubertal cumulus-oocyte complexes (COCs) at different meiotic stages after 24 h of culture.

Total	Degenerate DNA	GV	Metaphase I	Metaphase II	Total meiosis resumption
100 (n=204)	3.4 (n=7)	2.5 (n=5)	20.1 (n=41)	74.0 (n=151)	94.1 (n=192)

Table 4
Morphometric and fluorescence intensity measurements in adult and prepubertal ewe oocytes from antral follicles ≥3 mm in diameter (n=24 and 28 oocytes, respectively).

Variable	Ad	Pp	Significance ($p<$)
Cytoplasmic diameter (µm)	123.6±2.2	133.8±2.0	0.002
Morphometric features of GV			
Area (µm²)	1039.1±66.2	11298.7±61.3	0.004
EqD (µm)	36.5±1.1	40.5±1.0	0.005
Per (µm)	119.3±3.3	129.3±28.6	0.01
SF	0.960±0.003	0.973±0.003	0.001
Fluorescence features[1]			
TFI (× 10⁶)	30.7±2.8	49.6±2.6	0.0001
MinI	342.2±24.2	355.7±22.4	NS
MeanI	766.7±55.9	976.4±51.7	0.006
MaxI	3100.4±208.2	3787.3±192.8	0.016

Fluorescence features[1]: Expressed in arbitrary fluorescence units (AFU).
Morphometric and fluorescence intensity measurements are defined in the text, section 2.5.

The mean intensity and TFI of prepubertal GVs were higher than those of adult GVs (Table 4), however, despite this, the minimum intensity values observed in adult and prepubertal GVs were similar.

All the morphometric (Fig. 4 B–E) and fluorescence (Fig. 4: F, G, and I) features except minimum intensity, which was not different between the age groups (Fig. 4H), showed statistically higher values in the prepubertal group. The significant difference observed in fluorescence features was not completely due to differences in size, since it was also observed when morphometric variables were included in the models as covariates. Nevertheless, in spite of the significant differences found between adult and prepubertal oocytes in the size and fluorescence intensity of GVs, there was a clear overlap between both age groups, as shown in the box plots of the variables measured (Fig. 4). The most usual pattern of GV configuration found in the two age groups, irrespective of the size, was SNE. However, it was observed that in adult GVs, chromatin was condensed into distinct clumps or

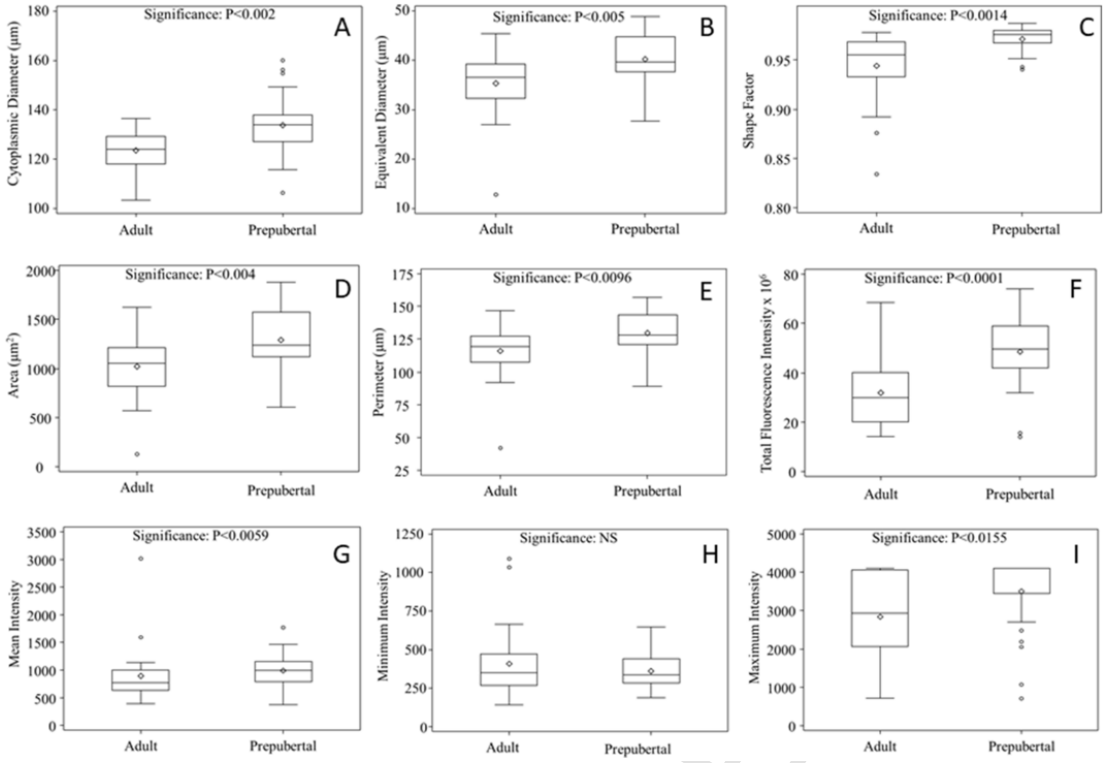

Fig. 4. Morphometric and fluorescence differences between adult and prepubertal oocytes represented as box-and-whiskers plots. A: Cytoplasmic diameters of adult and prepubertal oocytes. B–I: Morphometric and fluorescence features of GVs from adult and prepubertal sheep. The diamond symbol and the horizontal line in the box interior represent the group mean and median, respectively. The upper and lower ends of the box represent the first and third quartiles (25th and 75th percentiles, respectively) so that the length of the box represents the interquartile range (IQR). The upper and lower whiskers represent the highest and lowest observed values that are no higher and no lower than 1.5-times the IQR above and below the 75th and 25th percentiles, respectively. Open dots represent outliers (values higher or lower than the above-mentioned limits). Values higher or lower than three times the IQR above and below the 75th and 25th percentiles, respectively, were not observed in the present study.

clusters which were independent of each other (Suppl. Fig. 2C, 2 E, and 2 G). In contrast, the chromatin configuration of most prepubertal GVs was fibrillary and continuous (Suppl. Fig. 2 F and 2H). Among the prepubertal GVs, only one SNE showing the lowest TFI and a small size (Suppl. Fig. 2 B) also displayed condensed chromatin forming a typical ring around the nucleolus.

3.2.3. Differences in meiotic and developmental competence of adult and prepubertal oocytes

Follicular aspiration was more efficient in prepubertal than in adult ovaries (Table 5).Hence, although only ≥ 3 mm follicles were punctured in both age groups, the number of oocytes recovered that were suitable for IVM per ovary in prepubertal ewes was almost double the number recovered from in adult ewes. Meiotic resumption was similar in oocytes recovered from prepubertal and adult follicles, however, progression to MII was significantly higher in adult oocytes than in prepubertal oocytes (90 *vs* 57%, Table 5, Fig. 5 A). The difference in MI rate between adult and prepubertal oocytes (10.5 *vs* 14.3%) was not significant. Both groups showed similar cleavage rates at 24 and 48 h after IVF (Table 5, Fig. 5 B), however, development to the blastocyst stage was significantly higher ($p<0.0001$) for oocytes from adult ovaries than prepubertal ovaries (42% *vs* 8%). The kinetics of the development to blastocyst was faster in the adult group, since no blastocysts from prepubertal oocytes were observed at day 6 of culture, whereas 26% of the adult ewe group had reached this stage at this time point (Table 6).

Table 5
Meiotic competence of adult and prepubertal oocytes.

Age of ewes	Adult	Prepubertal	Significance ($p<$)
Number of ovaries	160	199	-
Number of grade 1 COCs	146	267	-
Number of COCs to IVM[a]	121	237	-
Number of COCs for meiotic competence[b]	19	28	-
% Deg. DNA	0 (0/19)	3.6 (1/28)	NS
% Meiosis resumption	**100 (19/19)**	**96.4 (27/28)**	**NS**
% Metaphase I	10.5 (2/19)	14.3 (4/28)	NS
% Metaphase-anaphase	0.0 (0/19)	25.0 (7/28)	0.0023
% Metaphase II	89.5 (17/19)	57.1 (16/28)	0.0057

NS: Not significant ($p>0.05$).

[a] A random sample of 25 adult and 30 prepubertal cumulus-oocyte complexes (COCs) was collected prior to *in vitro* maturation (IVM) to develop studies of chromatin configuration and global DNA methylation in germinal vesicle (GV) oocytes (Suppl. Fig. 2).

[b] Twenty adult and thirty IVM prepubertal oocytes were used as controls for meiotic competence after IVM (Fig. 5A); one adult and two lamb oocytes were destroyed during the processing of the samples.

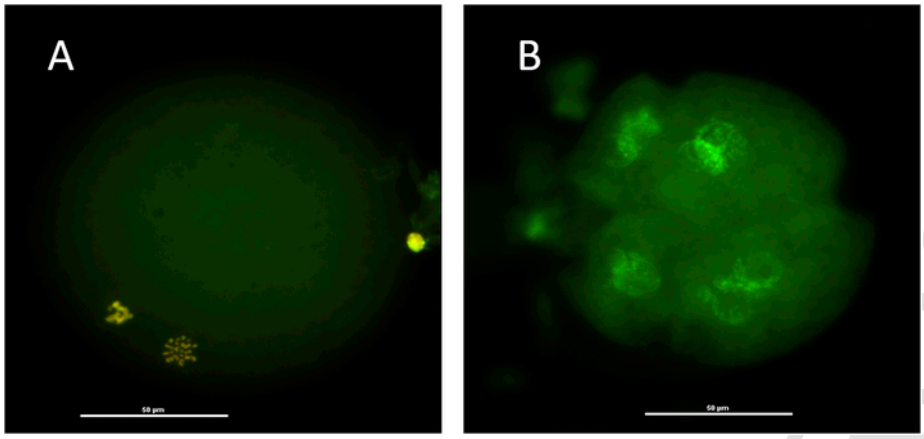

Fig. 5. Inverted epifluorescence images of: A: 5-methylcytosine immunolabeling after *in vitro* maturation showing metaphase II chromosomes and a polar body. B: 4–8 cell stage embryo 48 h after *in vitro* fertilization.

Table 6
In vitro developmental competence of prepubertal and adult oocytes after *in vitro* fertilization (IVF).

Age of ewes	Adult	Prepubertal	Significance ($p<$)
Number of COCs to IVF	101	203	-
% Cleaved 24 h	25.7 (26/101)	21.2 (43/203)	NS
% Cleaved 48 h	88.1 (89/101)	84.2 (171/203)	NS
% D6 blastocysts/Cleaved[a]	26.0 (20/77)	0.0 (0/151)	0.0001
% D7 blastocysts/Cleaved	14.3 (11/77)	5.3 (8/151)	0.04
% D8 blastocysts/Cleaved	1.3 (1/77)	2.6 (4/151)	NS
% Total Blastocysts/Cleaved	41.6 (32/77)	7.9 (12/151)	0.0001

[a] A random sample of 12 adult and 20 prepubertal cleaved embryos was collected to carry out studies of chromatin configuration and global DNA methylation (Fig. 5B).

4. Discussion

The use of oocytes obtained from prepubertal animals in IVP systems confers a significant advantage to accelerate genetic selection. However, recent articles have reported no 5-mC methylation staining in oocytes obtained at an early prepubertal age (1-month old) [10,11], which would hamper the application of these biotechnologies to breeding schemes. Our study on prepubertal oocyte morphology and functionality shows for the first time that the GVs of ovine oocytes from antral follicles ≥3 mm in diameter, obtained from 3-month-old donors, show global DNA methylation. Oocyte development during pre-puberty has not been characterized in sheep, however, age-related changes in global chromatin have been well documented in mice. In prepubertal mice, a high proportion of follicles reach the antral stage, and the number of NSN oocytes roughly equals that of SN oocytes, whereas in adult mice, the percentage of SN oocytes increases up to 90% [25]. Similarly, the immunofluorescence data on adult and prepubertal GVs presented herein show that the SNE chromatin configuration was established in most oocytes (98%) recovered from follicles≥ 3 mm from 3-month-old ewes and that global methylation, evidenced by the 5-mC signal, was observed in all GVs analyzed from both age groups, indicating that mature GVs were present in prepubertal oocytes, since DNA methylation plays a crucial role in many biological processes including genomic transcription [31]. In addition, 5-mC immunolabeling images of GVs provided direct evidence that the DNA methylation and nuclear architecture were similar in oocytes from adults and 3-month-old ewes when obtained from antral follicles ≥3 mm. Therefore, the prepubertal oocytes analyzed in this study present the pattern of chromatin configuration and DNA methylation typical of a fully mature gamete, as described by Russo et al. [24] for adult oocytes.

The nuclei of fully differentiated adult sheep oocytes start to display an inactive condensed chromatin configuration (SNE) and high levels of DNA methylation already in the late growing stage (≥110 μm) of early antral follicles [24,32]. In agreement with this, most of the oocytes recovered in our study, with a medium size of 124.7 ± 6.5 μm, showed a condensed chromatin SNE configuration irrespective of the donor's age. In contrast, the studies indicating incomplete nuclear maturation were carried out with earlier prepubertal oocytes with a diameter less than 110 μm [10], which provides a plausible explanation for the differences between the studies. In agreement with our results, Barboni et al. [33] also observed that nuclear-epigenetic maturation was equivalent in full-size oocytes grown under *in vivo* or *in vitro* conditions from preantral sheep follicles. More recently, Masala et al. [12] showed no differences in the global DNA methylation in fully grown oocytes from adult and 4-week-old donors. This latter article did not specify the fluorescence parameters and differences between adult and prepubertal ewes, however, it reported relevant information about methylation and hydroxymethylation during meiotic progression and the pronuclear stage.

The differences in chromatin configuration between prepubertal and adult oocytes were minimal when comparing GVs with similar sizes. Thus, although the GV median size parameters were higher in the prepubertal group than the adult group, and oocytes showed a higher degree of chromatin compaction in the adult group than the prepubertal group, a significant overlap in these parameters occurred between both groups and anti-5-mC staining was observed in all GVs analyzed, irrespective of donor age. However, although the SNE pattern was observed in GVs analyzed from both age groups, chromatin did not surround the nucleolus. It is possible that, at this stage of chromatin configuration when oocytes are transcriptionally silent, the nucleolus is not detectable, as has been reported in other species such as goats [34] and pigs [35]. Notably, in fully grown GV oocytes, the nucleolus has an unusual ultrastructure and function, and it is often referred to as a nucleolus-like body (NLB) [36].

In agreement with the overall normalcy of prepubertal GVs, most oocytes obtained from follicles ≥3 mm of prepubertal sheep were able to resume and complete meiotic maturation up to MII, as pre-

viously reported by Cecconi et al. [37]. Nevertheless, at the end of IVM culture, we observed that one fifth of the oocytes were still at MI or anaphase 1 (AI); this delay has also been observed by Ledda et al. [6] in ovine oocytes obtained at a younger age than those used in the present study. More recent research results have shown that the maturation and fertilization rates do not differ between prepubertal and adult oocytes, even though oocytes from 30 to 40-day-old donors reach MI stage 1 h later than adult oocytes. This delay increases as the first meiotic division proceeds [9]. The more compacted structure of the chromatin and the smaller GV size we observed mainly in oocytes from adult ovaries compared to the bigger size of prepubertal GVs when chromatin is fibrillary and continuous might also explain this delay, since DNA must acquire a much more compacted structure to achieve metaphase II [19].

In relation to developmental competence, although the global chromatin configuration and meiotic competence were grossly similar in the prepubertal and adult oocytes derived from antral follicles ≥3 mm, the blastocyst rates were much lower in the prepubertal group. Our results suggest that the lack of global DNA methylation is not the main cause for the reduced developmental potential of prepubertal oocytes from 3–4-month-old donors, which is in contrast to reports on younger donors [10].

Several pieces of evidence have demonstrated that the large-scale chromatin condensation described in several mammalian oocytes during the process of growth is correlated with the progressive repression of the oocyte-genome's global transcription, which is required in order to reach a complete developmental potential [21,24,38–40]. At the same time, the occurrence of cytosine methylation elicits in the oocyte a wide range of biological functions, including the reprogramming of the germ cell itself and the success of early embryo-fetal development. The relevance of DNA methylation for embryo development and offspring health has been clearly demonstrated [41,42]. Our results show a similarity in the chromatin pattern and global DNA methylation pattern between the nuclei of oocytes isolated from follicles ≥3 mm from adults and prepubertal ewes. Moreover, the big difference detected in developmental competence between oocytes from adult and ≥ 3-month-old ewes clearly demonstrates that the large-scale chromatin condensation and global DNA methylation, although necessary, are not enough to ensure oocyte developmental competence.

In the present work the *in vitro* maturation procedure was identical for prepubertal and adults COCs. It is likely that an optimization of this procedure would improve the developmental competence of prepubertal oocytes, since no remarkable epigenetic deficiencies were detected at the age referred to in the present work. During the last few years, many studies have been conducted to improve oocyte nuclear and cytoplasmic maturation through meiotic arrest maintenance [43]. Although limited progress has been achieved, a recent study reported a prolonged pre-maturation culture system that can maintain oocytes retrieved from unprimed prepubertal mice under meiotic arrest while promoting their acquisition of developmental competence [44]. More recently, another study revealed that meiotic arrest enhances the developmental potential of both prepubertal NSN and adult SN oocytes, and that oocyte cytoplasmic maturation is correlated with gene transcription but not with chromatin condensation [45]. In line with these articles, the delay in *in vitro* nuclear maturation detected in the prepubertal oocytes suggests that, instead of strategies aiming to increase DNA methylation, meiotic arrest maintenance constitutes a promising strategy to enhance the developmental competence of prepubertal ovine oocytes.

In summary, our results demonstrate that adult-size oocytes from 3-month-old ewe lamb donors show genome-wide methylation and a chromatin configuration similar to that of adult oocytes obtained from follicles≥ 3 mm, therefore, they might be a valuable source of biological material for *in vitro* reproduction studies, although advances are required to improve oocyte *in vitro* maturation and developmental competence.

Declaration of interest

The authors declare no conflicts of interest.

Funding

This work was funded was suportad by INIA, Spanish Ministry of Economy and Competitiveness (RTA2011-00128-C02 and RTA2013-00041-C02).

Acknowledgements

We thank R. Mozo and E. Echegoyen for collecting the ovaries used in the experiments.

Appendix A. Supplementary data

Supplementary data to this article can be found online at https://doi.org/10.1016/j.theriogenology.2019.07.011.

References

[1] Y. Cognié, N. Poulin, Locatelli, P. Mermillod, State-of-the art production, conservation and transfer of in-vitro-produced embryos in small ruminants, Reprod Fertil Dev 16 (2004) 437–445.
[2] K. Gou, H. Guan, J. Bai, X. Cui, Z. Wu, F.X. Yan, X.R. An, Field evaluation of juvenile in vitro embryo transfer (JIVET) in sheep, Anim Reprod Sci 112 (2009) 316–324.
[3] G.S. Amiridis, S. Cseh, Assisted reproductive technologies in the reproductive management of small ruminants, Anim Reprod Sci 130 (2012) 152–161.
[4] J.K. O'Brien, S.L. Catt, K.A. Ireland, W.M.C. Maxwell, G. Evans, In vitro and in vivo developmental capacity of oocytes from prepubertal and adult sheep, Theriogenology 47 (1997) 1433–1443.
[5] G. Ptak, P. Loi, M. Dattena, M. Tischner, P. Cappai, Offspring from one-month-old lambs: studies on the developmental capability of prepubertal oocytes, Biol Reprod 61 (1999) 1568–1574.
[6] S. Ledda, L. Bogliolo, P. Calvia, G. Leoni, S. Naitana, Meiotic progression and developmental competence of oocytes collected from juvenile and adult ewes, J Reprod Fertil 109 (1997) 73–78.
[7] K.M. Morton, S.L. Catt, W.M.C. Maxwell, G. Evans, Effects of lamb age, hormone stimulation and response to hormone stimulation on the yield and in vitro developmental competence of prepubertal lamb oocytes, Reprod Fertil Dev 17 (2005) 593–601.
[8] G. Leoni, Succu S. Bebbere, F. Berlinguer, F. Mossa, M. Galioto, L. Bogliolo, S. Ledda, S. Naitana, Relations between relative mRNA abundance and developmental competence of ovine oocytes, Mol Reprod Dev 74 (2007) 249–257.
[9] G.G. Leoni, M.G. Palmerini, V. Satta, S. Succu, V. Pasciu, A. Zinellu, C. Carru, G. Macchiarelli, S.A. Nottola, S. Naitana, F. Berlinguer, Differences in the kinetic of the first meiotic division and in active mitochondrial distribution between prepubertal and adult oocytes mirror differences in their developmental competence in a sheep model, PLoS One 10 (4) (2015), e0124911.
[10] G. Ptak, K. Matsukawa, C. Palmieri, L. Della Salda, P.A. Scapolo, P. Loi, Developmental and functional evidence of nuclear immaturity in prepubertal oocytes, Hum Reprod 21 (2006) 2228–2237.
[11] Y. Fang, X. Zhang, J. Zhang, R. Zhong, D. Zhou, Global DNA methylation and related mRNA profiles in sheep oocytes and early embryos derived from pre-pubertal and adult donor, Anim Reprod Sci 164 (2016) 144–151.
[12] L. Masala, G.P. Burrai, E. Bellu, F. Ariu, L. Bogliolo, S. Ledda, D. Bebbere, Methylation dynamics during folliculogenesis and early embryo development in sheep, Reproduction 153 (2017) 605–619.
[13] K. Zhang, G.W. Smith, Maternal control of early embryogenesis in mammals, Reprod Fertil Dev 27 (2015) 880–896.
[14] V. Lodde, S. Modina, P. Maddox-Hyttel, F. Franciosi, A. Lauria, A.M. Luciano, Oocyte morphology and transcriptional silencing in relation to chromatin remod-

eling during the final phases of bovine oocyte growth, Mol Reprod Dev 75 (2008) 915–924.
[15] A.M. Luciano, V. Lodde, Changes of large-scale chromatin configuration during mammalian oocyte differentiation, in: G. Coticchio, D. Albertini, L. De Santis (Eds.), Oogenesis, Springer-Verlag, London, 2013, pp. 93–108.
[16] J.H. Crichton, C.J. Playfoot, I.R. Adams, The role of chromatin modifications in progression through mouse meiotic prophase, J Genet Genom 41 (2014) 97–106.
[17] F. Sánchez, J. Smitz, Molecular control of oogenesis, Biochim Biophys Acta 1822 (2012) 1896–1912.
[18] K.R. Stewart, L. Veselovska, G. Kelsey, Establishment and functions of DNA methylation in the germline, Epigenomics 8 (2016) 1399–1413.
[19] J.H. Crichton, C.J. Playfoo, I. Adams, The role of chromatin modifications in progression through mouse meiotic prophase, J Genet Genom 41 (2014) 97–106.
[20] M. Zuccotti, V. Merico, S. Cecconi, C.A. Redi, S. Garagna, What does it take to make a developmentally competent mammalian egg?, Hum Reprod Update 17 (2011) 525–540.
[21] R. De La Fuente, Chromatin modifications in the germinal vesicle (GV) of mammalian oocytes, Dev Biol 292 (2006) 1–12.
[22] R. De La Fuente, C. Baumann, M.M. Viveiros, Epigenetic modifications during mammalian oogenesis: emerging roles of chromatin structure during oocyte growth and meiotic maturation, in: A.K. Naumova, T. Taketo (Eds.), Epigenetics in human reproduction and development, World Scientific Publishing, London, 2017, pp. 35–58.
[23] A. Luciano, F. Franciosi, C. Dieci, V. Lodde, Changes in large-scale chromatin structure and function during oogenesis: a journey in company with follicular cells, Anim Reprod Sci 149 (2014) 3–10.
[24] V. Russo, A. Martelli, A. Mauro, P. Berardinelli, O. Di Giacinto, N. Bernabò, D. Fantasia, Barboni B. Mattioli, Modifications in chromatin morphology and organization during sheep oogenesis, Microsc Res Tech 70 (2007) 733–744.
[25] M. Zuccotti, S. Grana, V. Merico, M. Monti, C.A. Red, Chromatin organisation and nuclear architecture in growing mouse oocytes, Mol Cell Endocrinol 234 (2005) 11–17.
[26] J.H. Tan, H.L. Wang, X.S. Sun, Y. Liu, H.S. Sui, J. Zhang, Chromatin configurations in the germinal vesicle of mammalian oocytes, Mol Hum Reprod 15 (2009) 1–9.
[27] M.J. Cocero, J. Alabart, S. Hammami, J. Martí, B. Lahoz, P. Sanchez, E. Echegoyen, J.F. Beckers, J. Folch, The efficiency of in vitro ovine embryo production using an undefined or a defined maturation medium is determined by the source of the oocyte, Reprod Domest Anim 46 (2011) 463–470.
[28] F. Santos, W. Dean, Using immunofluorescence to observe methylation changes in mammalian preimplantation embryos changes in mammalian preimplantation embryos, Methods Mol Biol 325 (2006) 129–137.
[29] Nikon NIS-elements documentation user's guide (ver. 3.12), Laboratory Imaging s.r.o., Za Drahou 171/17, CZ - 102 00 Praha, vol. 10, 2009.
[30] SAS Institute Inc, SAS/STAT® 14.1 user's guide, SAS Institute Inc, Cary, NC, 2015.
[31] R. Jaenisch, A. Bird, Epigenetic regulation of gene expression: how the genome integrates intrinsic and environmental signals, Nat Genet 33 (Suppl) (2003) 245–254.
[32] V. Russo, N. Bernabò, O. Di Giacinto, A. Martelli, A. Mauro, P. Berardinelli, V. Curini, D. Nardinocchi, M. Mattioli, B. Barboni, H3K9 trimethylation precedes DNA methylation during sheep oogenesis: DAC1, SUV39H1, G9a, HP1, and Dnmts are involved in these epigenetic events, J Histochem Cytochem 61 (2013) 75–89.
[33] B. Barboni, V. Russo, S. Cecconi, V. Curini, A. Colosimo, M.L.A. Garofalom, G. Capacchietti, O. Di Giacinto, M. Mattioli, In vitro grown sheep preantral follicles yield oocytes with normal nuclear-epigenetic maturation, PLoS One 6 (2011), e27550.
[34] H.S. Sui, Y. Liu, D.Q. Miao, J.H. Yuan, T.W. Qiao, M.J. Luo, J.H. Tan, Configurations of germinal vesicle (GV) chromatin in the goat differ from those of other species, Mol Reprod Dev 71 (2005) 227–236.
[35] M.J. Sun, S. Zhu, Y.W. Li, J. Lin, S. Gong, G.Z. Jiao, F. Chen, J.H. Tan, An essential role for the intra oocyte MAPK activity in the NSN to-SN transition of germinal vesicle chromatin configuration in porcine oocytes, Sci Rep 6 (2016) 23555.
[36] C. Bouniol-Baly, L. Hamraoui, J. Guibert, N. Beaujean, M.S. Szollosi, J. Cohen, H. Malter, C. Elsner, H. Kort, J. Massey, M.P. Mayer, Immunosuppression supports implantation of zona pellucida dissected human embryos, Fertil Steril 54 (1990) 662–665.
[37] S. Cecconi, A. Mauro, G. Capacchietti, P. Berardinelli, N. Bernabo, A.R. Di Vincenzo, M. Mattioli, B. Barboni, Meiotic maturation of incompetent prepubertal sheep oocytes is induced by paracrine factor(s) released by gonadotropin-stimulated oocyte-cumulus cell complexes and involves mitogen-activated protein kinase activation, Endocrinology 149 (2008) 100–107.
[38] C. Bouniol-Baly, L. Hamraoui, J. Guibert, N. Beaujean, M.S. Szollosi, et al., Differential transcriptional activity associated with chromatin configuration in fully grown mouse germinal vesicle oocytes, Biol Reprod 60 (1999) 580–587.
[39] W. Dean, D. Lucifero, F. Santos, DNA methylation in mammalian development and disease, Birth Defects Res 75 (2005) 98–111.
[40] V. Lodde, S. Modina, C. Galbusera, F. Franciosi, A.M. Luciano, Large-scale chromatin remodeling in germinal vesicle bovine oocytes: interplay with gap junction functionality and developmental competence, Mol Reprod Dev 74 (2007) 740–749.
[41] S. Bao, Y. Obata, J. Carroll, I. Domeki, T. Kono, Epigenetic modifications necessary for normal development are established during oocyte growth in mice, Biol Reprod 62 (2000) 616–621.
[42] A.K. Swales, N. Spears, Genomic imprinting and reproduction, Reproduction 130 (2005) 389–399.
[43] M. Conti, F. Franciosi, Acquisition of oocyte competence to develop as an embryo: integrated nuclear and cytoplasmic events, Hum Reprod Update 24 (2018) 245–266.
[44] S. Romero, F. Sánchez, F. Lolicato, H. Van Ranst, J. Smitz, Immature oocytes from unprimed juvenile mice become a valuable source for embryo production when using C-type natriuretic peptide as essential component of culture medium, Biol Reprod 95 (2016) 64.
[45] F. Chen, J. Lin, X. Sun, B. Xiao, S.F. Ning, S. Zhu, H.-L. Wang, J.-H. Tan, Mechanisms by which in vitro meiotic arrest and sexual maturity improve developmental potential of mouse oocytes, Sci Rep 7 (2017) 15763.